



Original Article

Extracts of *Portulaca oleracea* promote wound healing by enhancing angiology regeneration and inhibiting iron accumulation in mice

Jinglin Guo^a, Juan Peng^b, Jing Han^a, Ke Wang^c, Ruijuan Si^a, Hui Shan^a, Xiaoying Wang^a, Ju Zhang^{a,*}

^a School of Nursing, Qingdao University, Qingdao 266071, China

^b Surgery of Traditional Chinese Medicine, Second Affiliated Hospital of Tianjin University of Traditional Chinese Medicine, Tianjin 300150, China

^c School of Pharmacy, Qingdao University, Qingdao 266071, China

ARTICLE INFO

Article history:

Received 8 August 2021

Revised 24 September 2021

Accepted 30 September 2021

Available online 26 February 2022

Keywords:

deep tissue pressure injur

ischemia-reperfusion

Portulaca oleracea L.

tissue repair

wound healing

ABSTRACT

Objective: To investigate the role of *Portulaca oleracea* (POL) in promoting revascularization and re-epithelization as well as inhibiting iron aggregation and inflammation of deep tissue pressure injury (DTPI).

Methods: The hydroalcoholic extract of POL (P) and aqueous phase fraction of POL (PD) were prepared based on maceration and liquid–liquid extraction. The number of new blood vessels and VEGF-A expression level were assessed using H&E stain and Western blot on injured muscle to examine the role of POL different extracts in vascularization. The iron distribution and total elemental iron of injured muscle were detected using laser ablation inductively coupled plasma mass spectrometry (ICP-MS) and Perls' staining to determine whether POL extracts can inhibit the iron accumulation. Besides, the ability of POL extracts to promote wound healing by combining re-epithelization time, inflammation degree and collagen deposition area were comprehensively evaluated.

Results: *In vitro*, we observed a significant increase in HUVEC cell viability, migration rate and the number of the tube after P and PD treatment ($P < 0.05$). *In vivo*, administration of P and PD impacted vascularization and iron accumulation on injured tissue, evident from more new blood vessels, higher expression of VEGF-A and decreased muscle iron concentration of treatment groups compared with no-treatment groups ($P < 0.05$). Besides, shorter re-epithelization time, reduced inflammatory infiltration and distinct collagen deposition were associated with administration of P and PD ($P < 0.05$).

Conclusion: POL extract administration groups have high-quality wound healing, which is associated with increased new blood vessels, collagen deposition and re-epithelization, along with decreased iron accumulation and inflammatory infiltration. Our results suggest that that POL extract is beneficial to repair injured muscle after ischemia–reperfusion, highlighting the potential of POL in the DTPI treatment.

© 2022 Tianjin Press of Chinese Herbal Medicines. Published by ELSEVIER B.V. This is an open access article under the CC BY-NC-ND license (<http://creativecommons.org/licenses/by-nc-nd/4.0/>).

1. Introduction

Approximately 1%–2% of the world's population suffer from chronic wounds, which bring pain, disability, and high medical costs (Frykberg & Banks, 2015). In the USA, the total cost for chronic wound management was estimated to range from \$28.1 to \$96.8 billion in 2014 (Vogt et al., 2020). Chronic wounds include diabetic ulcers, vascular ulcers and pressure ulcers. Deep tissue pressure injury (DTPI) is a severe pressure ulcer with a high concealment characteristic in addition to rapid deterioration, pain, high morbidity, and low rate of healing (Liu et al., 2020). DTPI often occurs in older individuals with cardiovascular disorders, dyskine-

sia, obesity, and diabetes, which inevitably results in a burden on familial resources and healthcare systems (Preston, Rao, Strauss, Stamm & Zalman, 2017).

Efficacious clinical treatments for DTPI are still lacking (Frykberg & Banks, 2015; Black & Berke, 2020). *Portulaca oleracea* L. (POL) has been used to treat wounds for thousands of years because of its wide distribution and low price. POL belongs to the Portulacaceae family of plants, which is an edible and medicinal herb. As a kind of food, POL possesses a source of nutrients, such as vitamin, β -carotene, γ -linoleic acid, omega-3 fatty acid, and minerals (Yang et al., 2016; Lee, Oh, Kong & Seo, 2019). Meanwhile, POL as a kind of medicine contains diverse active compounds, including terpenoids, flavonoids, alkaloids, coumarins and cerebroside (Baradaran Rahimi, Mousavi, Haghghi, Soheili-Far & Askari, 2019; Qiao et al., 2019). These active compounds provide

* Corresponding author.

E-mail address: zhangju111@qdu.edu.cn (J. Zhang).

extensive pharmacological effects, including neuroprotective, hepatoprotective, antiaging, antioxidative, antibleeding, analgesic, and anti-inflammatory activities (Qiao et al., 2019; Zheng et al., 2018). According to the records of Chinese Pharmacopoeia, POL is mainly used to treat stomach illnesses, liver disease, respiratory diseases, fever, headache, diarrhea, and ulcerative wound (Zhou et al., 2015; Iranshahy et al., 2017; Tao et al., 2018). It has been reported that the crude extract of POL could accelerate wound healing by decreasing the surface area of the wound and increasing the tensile strength (Rashed, Affi & Disi, 2003). The introduction of POL preparations for DTPI or chronic wound healing could reduce treatment costs whilst being readily accessible and accepted by elderly patients. However, there have been no reports exploring the effect of POL extracts on DTPI wound healing until now. In the present study, we prepared five kinds of extracts from POL, and the capability of each POL extract promoting DTPI wound healing was investigated using *in vitro* and *in vivo* experiments.

2. Materials and methods

2.1. Plant materials, primary reagents and kits

Dry leaves of POL were purchased from Beijing Tong Ren Tang (Beijing, China). Ethanol (95%), petroleum ether, ethyl acetate, and *n*-butane were obtained from Shanghai Macklin Biochemical (Shanghai, China). Human umbilical vein endothelial cell (HUVEC)-complete medium, Dulbecco's modified Eagle's medium (DMEM), fetal bovine serum (FBS), phosphate-buffered saline (PBS), penicillin–streptomycin solution, and dimethyl sulfoxide (DMSO) reagents were obtained from Procell Life Science and Technology (Wuhan, China). Hematoxylin and eosin (H&E) staining kit, Masson's trichrome staining kit, Perls' stain kit, and Pierce BCA protein assay kit were obtained from Wanleibio (Shenyang, China).

2.2. Animals

Male C57BL/6J mice (9 weeks, 20–22 g) were purchased from Beijing Vital River Laboratory Animal Technology (Beijing, China). Mice were housed at room temperature (about 22 °C), kept at 55% relative humidity and under a 12:12 h light–dark cycle. Mice were acclimatized for one week prior to experimentation and were provided a standard laboratory pellet diet and access to water during the study. The research was conducted in accordance with the internationally accepted principles for laboratory animal use and care as found in the European Community guidelines (EEC Directive of 1986; 86/609/EEC). Moreover, the research was executed in accordance with ethical guidelines approved by the Ethical Committee of Qingdao University (20201120C576520201226017).

2.3. Preparation of POL extracts

Five POL extracts were prepared according to previous protocols (Mekonnen et al., 2013). In brief, extracts were prepared based on maceration and liquid–liquid extraction. First, dry leaves of POL (990 g) was soaked in ethanol (95%) at room temperature (22–24 °C) for 7 d. The ethanol was replaced with fresh ethanol until the solution color changed from dark green to colorless (approximately 15 L ethanol (95%) was required). The POL powder residue was filtered and discarded, and the remained ethanol solution was collected. The ethanol was rotationally evaporated (N-1300, EYELA, Shanghai, China). The extract was freeze-dried (Alpha 2–4 LD plus, Christ, Beijing, China), to obtain approximately 112.5 g of hydroalcoholic extract of POL (P). Next, 110 g P was dispersed within 1 L distilled water, followed by fractionated sequentially with 1 L petroleum ether (fraction PA), 1 L ethyl acetate (fraction PB) and 1 L *n*-

butane (fraction PC). The remaining aqueous solution was collected as fraction PD. The four-phase fractions were concentrated by rotary evaporation and then freeze-dried (Fig. 1). The yield of P, PA, PB, PC and PD was 11.4%, 2.5%, 0.6%, 2.8% and 4.9% (mass percentage), respectively.

2.4. Preparation of working solution

For *in vitro* experiments, the five POL extracts (P, PA, PB, PC and PD) were dissolved in DMSO and then diluted with DMEM, ensuring that the concentration of DMSO in the final solution was <5%. The solutions were filtered by 0.22 µm pore sterile filter membranes and then prepared into diluents at 25, 50, 100, and 200 µg/mL concentrations. In *in vivo* experiments, P was dissolved in DMSO and then diluted to 8 mg/mL with distilled water. PD was diluted to 3, 6 and 12 mg/mL using distilled water.

2.5. *In vitro* cell studies

2.5.1. Cell culture

Human keratinocytes (HaCaT) were purchased from Wanlei Life Sciences (Shenyang, China) and cultured in DMEM medium supplemented with 10% FBS and 1% penicillin–streptomycin. Human endothelial cells (HUVEC) were gifted from the Chinese Academy of Medical Sciences & Peking Union Medical College Institute of Biomedical Engineering and cultured in an HUVEC-complete medium. The complete medium contained 10% FBS, 1% endothelial cell growth supplement and 1% penicillin–streptomycin. Cells were cultured in a humidified incubator at 37 °C with 5% CO₂.

2.5.2. CCK-8 assay

The effect of POL extracts on HaCaT and HUVEC viability and proliferation was estimated using CCK-8 assay. HaCaT and HUVEC cells (1×10^5 cells/well) were seeded in a 96-well plate. The working solution concentrations ranged from 25 to 200 µg/mL, and each concentration was used in a set of six parallel wells. Cells were respectively incubated for 24, 48, and 72 h before the addition of CCK-8 reagent and measurement of absorbance values at 450 nm using a microplate reader (PT-3502C, Potentov). The control group contained untreated cells.

2.5.3. Tube formation assay

Before the experiment, the 96-well plate was coated with Matrigel (50 µL/well) and incubated for 30 min at 37 °C. HUVECs (1×10^5 cells/well) were suspended in a serum-free culture medium containing different concentrations of working solution of P, PA, PB, PC and PD and then seeded on the Matrigel-coated 96-well plates. Each concentration was used in a set of three parallel wells. The cell suspension of the control group did not contain POL treatment (Meng et al., 2017). The number of tubes formed were observed under a microscope and photographed at the indicated time points. According to the results of the CCK-8 assay, the concentrations of P ranged from 25 to 200 µg/mL. Moreover, the PA, PB, PC and PD concentrations were set at 25 µg/mL.

2.5.4. Cell migration assay

HUVECs (5×10^5 cells/well) were cultured in a six-well plate until complete confluence. The complete medium containing different P, PA, PB, PC and PD concentrations were added to separate wells. The control group received a complete medium without POL extract (Wang et al., 2020). Under an inverted microscope, photographs were taken at 0, 12 and 24 h after a scratch-wound was made using a pipette tip. The cell-free area of each group at 0 h was taken as the original scratch/wound area. The scratch/wound closure percentage was calculated using the following equation:

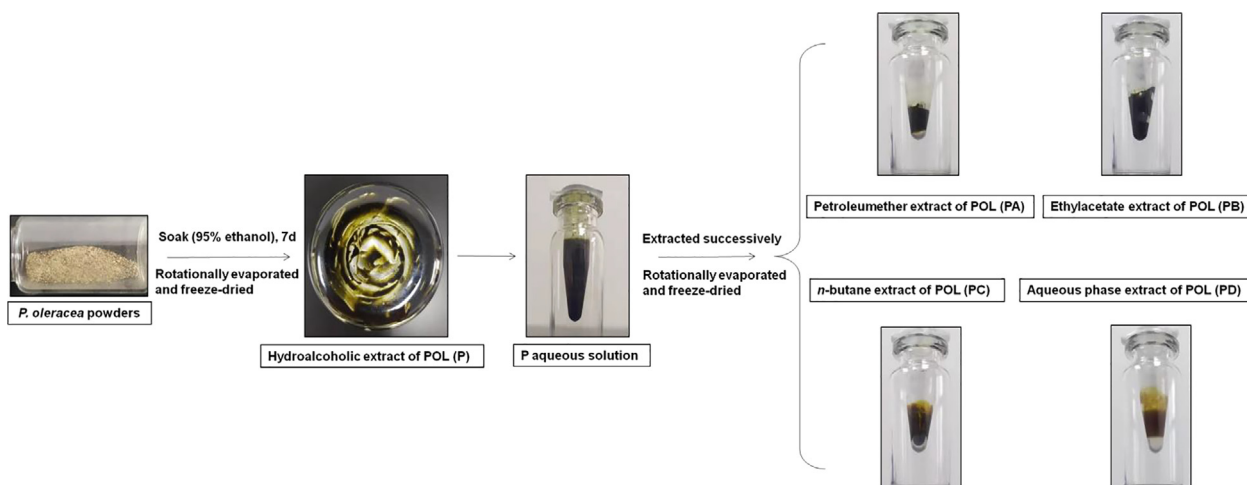


Fig. 1. Schematic diagram represented process of preparing five POL extracts.

Wound area (%) = (wound area at each time point/original wound area) \times 100.

2.6. In vivo wound healing assay

2.6.1. Construction of deep tissue pressure injury (DTPI) model

The DTPI model construction consulted previous literature (Liu et al., 2020). Hairs near the ischium spinout were shaved. Magnets (12 mm in diameter, 5 mm thickness, 2.4 g weight, 1000 G in surface magnetic flux) were placed on the upper and lower sides of the ischium spinout for pressure application. One pressure cycle is composed of pressure for 12 h followed by a release for 12 h. After 24 h, the time point was set as the first day of the experiment. Mice were fed typically during the pressure application and could move around freely.

2.6.2. Experimental grouping and wound treatment

The mice were randomly divided into five groups ($n = 15$ in each group): DTPI group (received 0.2 mL/d distilled water); P group (received 80 mg/kg·d⁻¹P); PD_L (low) group (received 30 mg/kg·d⁻¹PD); PD_M (medium) group (received 60 mg/kg·d⁻¹PD); and PD_H (high) group (received 120 mg/kg·d⁻¹PD). In addition, the normal group ($n = 5$) did not receive any pressure treatment or intervention. Dose parameters and administration modes were chosen based on previous studies (Qiao et al., 2019, Boskabady et al., 2019, Pakdel et al., 2019). The therapeutic effects of the different treatment groups were observed following intragastrical administration.

2.6.3. Wound healing evaluation

The developed wounds were photographed on 0, 1, 3, 5, 7, 9, 11, 13, 15, 17, 19 and 21 d. A specific ruler as a calibrator was utilized. The wound area at each time point was quantified by Image J software (NIH, USA). The wound area on the third day was taken as the original wound area due to the absence of an open wound before day 3. The percentage of the wound area was calculated using the following equation: Wound area (%) = (wound area at each time point/original wound area) \times 100.

2.6.4. Histopathological examination

Three mice were sacrificed on 7, 14 and 21 d, respectively. The skin and muscle around the wound within 1 cm² were isolated and post-fixed in cold paraformaldehyde (4%) solution. The isolated wound tissues were entrenched in paraffin film and divided into 5 μ m sections. Then, routine staining with H&E, Masson's tri-

chrome (MT) and Perls' stain were performed to reveal the morphological features of the wound, including the thickness of the epithelium, the density of new capillaries and appendages, the inflammatory infiltration degree, collagen deposition area and iron deposition.

2.6.5. Tissue iron concentration examination

The muscle below the wound within 1 cm² was isolated and dried at 95 °C for 3 d. Then, the muscle was accurately weighed and homogenized. According to the previous literature methods, inductively coupled plasma mass spectrometry (ICP-MS) was used to analyze the iron concentration of the homogenized muscle (Jensen et al., 2021, Alves et al., 2021)

2.6.6. Western blot

Wound site muscle tissue was washed twice with ice-cold PBS, and then the concentrations of VEGF-A and MMP-9 were determined using Pierce BCA protein assay kits according to the manufacturer's instructions. In brief, protein extracts were added to SDS-PAGE gels and separated by gel electrophoresis. The gels were blotted onto a nitrocellulose membrane and incubated with primary antibodies, using the following specific antibodies and concentrations: VEGF-A, MMP-9 (1:500) and GAPDH (1:1000). The protein expression was visualized with specific horseradish peroxidase (HRP)-conjugated secondary antibody. Then, a gel image processing system was used to analyze the semi-quantitative densitometry of target protein bands. GAPDH was used as a standard for the normalization of protein expression.

2.7. Statistical analysis

All data were expressed as mean \pm standard deviation (SD), and statistical analysis was performed using GraphPad Prism 7.0 software. Comparisons between two independent groups were conducted using the Student's *t*-test, and comparisons across multiple groups were conducted using One-way analysis of variance (ANOVA) and Tukey's multiple comparisons test. Significance was set at $P < 0.05$.

3. Results

3.1. Biocompatibility analysis of P and PD

All concentrations of P did not significantly decrease the viability of HaCaT cells over 24, 48 and 72 h (Fig. 2A – C). In the concen-

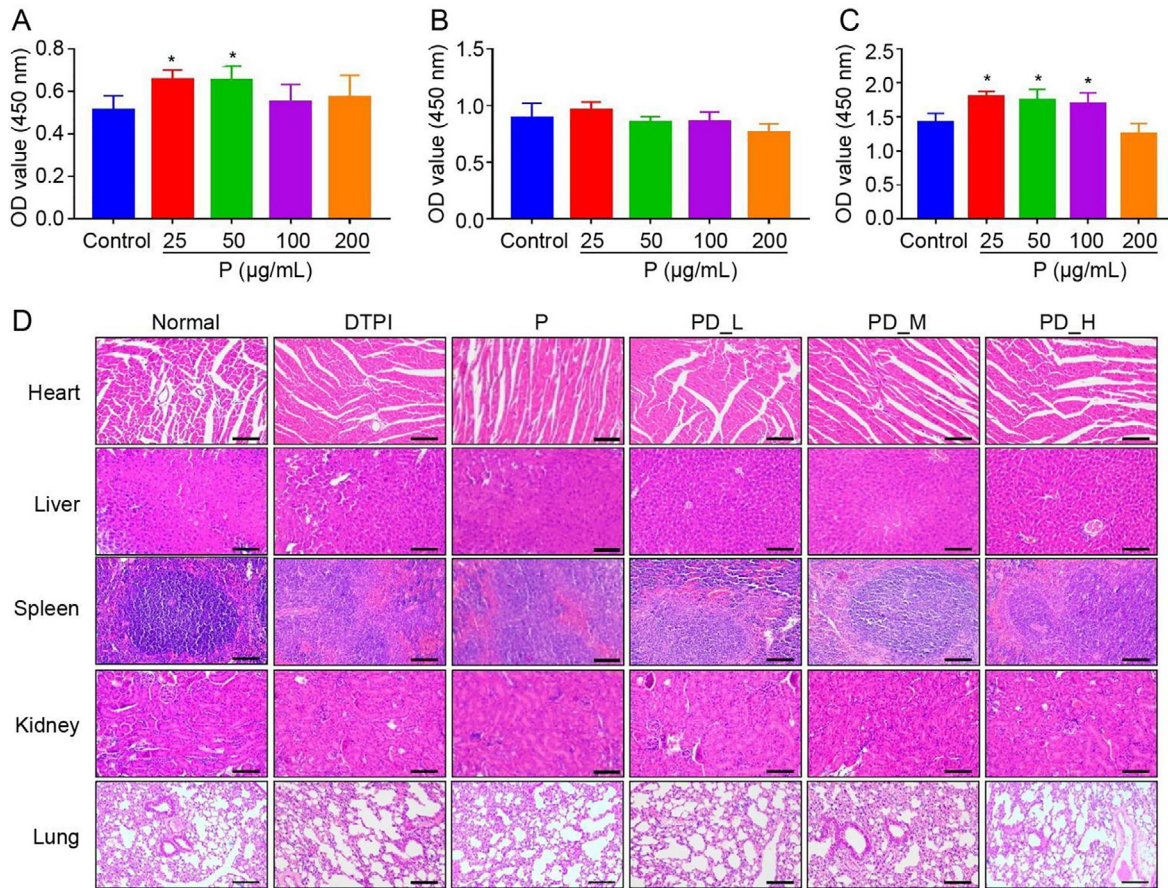


Fig. 2. Biocompatibility analysis of P on viability of HaCaT cells over 24 h (A), 48 h (B) and 72 h (C) by CCK-8 assays. (D) Effect of P and PD on pathological changes of main organs (heart, liver, spleen, kidney and lung) by HE staining ($\times 40$). Scale bar: 500 μm . Data presented as means \pm SD. * $P < 0.05$ vs control group.

tration range of 25–100 $\mu\text{g/mL}$, extract P significantly enhanced cell growth ($P < 0.05$) at 72 h compared to that in the control group. After 14 d of intragastric administration by oral intake, the pathological structure of significant organs in the P and PD group mice showed no noticeable pathological changes compared to organs in the normal (untreated) group (Fig. 2D).

3.2. P and PD benefit HUVEC cells proliferation, angiogenesis and migration

As shown in Fig. 3A, extract P did not inhibit HUVEC proliferation compared with the control group at 48 and 72 h ($P > 0.05$), besides, P used at 25 and 50 $\mu\text{g/mL}$ significantly enhanced cell proliferation at 24 ($P < 0.05$). Specifically, the fraction extract PA at concentrations 25 and 50 $\mu\text{g/mL}$ significantly promoted cell proliferation at 24 h compared with the control group ($P < 0.05$) but showed no significant changes after that ($P > 0.05$). In addition, PA at 100 and 200 $\mu\text{g/mL}$ showed inhibition of cell proliferation at 72 h and all-time points compared with the control group, respectively ($P < 0.05$) (Fig. 3B). On the contrary, the extracts PB and PC were averse to HUVEC proliferation, and all concentrations of PB and PC showed reduced cell viability at 72 h compared with the control group ($P < 0.05$) (Fig. 3C and D). Additionally, 25 and 50 $\mu\text{g/mL}$ of PD had beneficial effects on cell proliferation, but a high concentration (200 $\mu\text{g/mL}$) of PD was unfavorable to cell proliferation compared with the control group ($P < 0.05$) (Fig. 3E). Comparisons of OD values of P and PD at three-time points showed

that at 72 h, the cells in the PD (25 $\mu\text{g/mL}$) group had highest viability than those in control, PD (50 $\mu\text{g/mL}$) and P (25 and 50 $\mu\text{g/mL}$) groups ($P < 0.05$) (Fig. 3F).

For tube formation assays, the concentrations of PA, PB, PC and PD were set at 25 $\mu\text{g/mL}$ because this concentration was most beneficial to promote cell proliferation. We found that the number of tubes in the P groups (25–200 $\mu\text{g/mL}$) were consistently more than that in the control group at 30 and 36 h ($P < 0.05$) (Fig. 4A and B). As Fig. 4C and D showed, the number of tubes in PA, PB, PC, and PD groups were also significantly higher than that in the control group at 30 and 36 h ($P < 0.05$). However, the number of tubes in the PC group was fewer than that in the other three extracts groups at 30 and 36 h ($P < 0.05$).

The migration ability of HUVEC was assessed. We observed that the migration ability of HUVEC was assessed. We observed that the scratch-wound area in the 25 and 50 $\mu\text{g/mL}$ P groups decreased significantly at 12 h and 24 h compared with the control group ($P < 0.05$). Moreover, there was no significant difference in wound closure rates between the P (100 $\mu\text{g/mL}$) group and the control group ($P > 0.05$). Besides, P at 200 $\mu\text{g/mL}$ was detrimental to scratch-wound closure owing to excessive concentration (200 $\mu\text{g/mL}$) was toxic to cells ($P < 0.05$) (Fig. 5A and B). Compared with the control group, the fraction extracts, PA and PD, showed significantly lower percentages of the remaining wound area, suggesting enhanced migration at 12 and 24 h time points ($P < 0.05$). Fraction extracts PB and PC showed no significant differences compared to the migration rates of the control group ($P > 0.05$) (Fig. 5C and D).

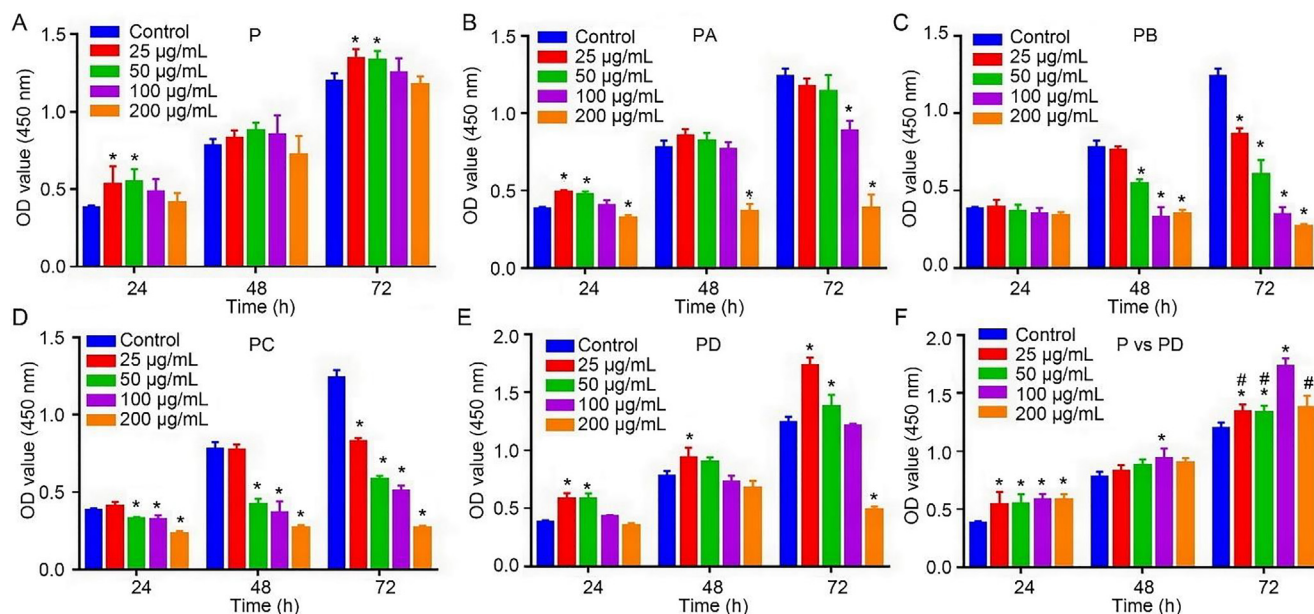


Fig. 3. POL extracts promoted revascularization and wound healing *in vitro*. P, PA and PD promoted cell proliferation in a concentration-dependent manner. (A – E) Effect of different extracts (P, PA, PB, PC and PD) on cell proliferation by CCK-8 assay. (F) Comparative results of P and PD in promoting cell proliferation. Data presented as means ± SD. **P* < 0.05, vs control group, #*P* < 0.05, vs PD (25 µg/mL) group.

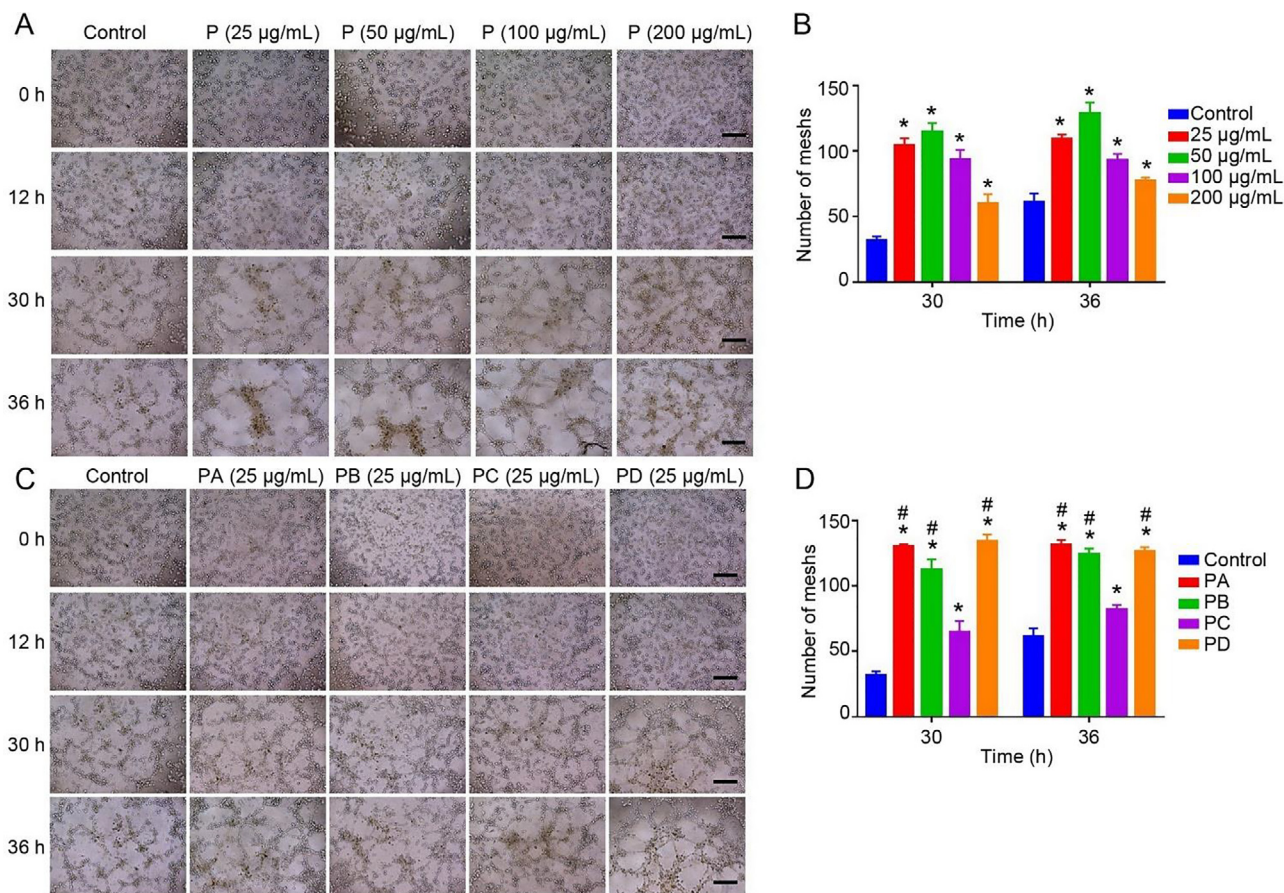


Fig. 4. P, PA, PB, PC and PD were benefited to HUVEC tube formation. (A) Tube formation images in the control group and different concentrations of P groups (×100). (B) Quantitative analysis of the number of tubes in A. (C) Tube formation images in control, PA, PB, PC and PD groups (×100). (D) Quantitative analysis of the number of tubes in C. Scale bar: 200 µm. Data presented as means ± SD. **P* < 0.05 vs control group, #*P* < 0.05 vs PC group.

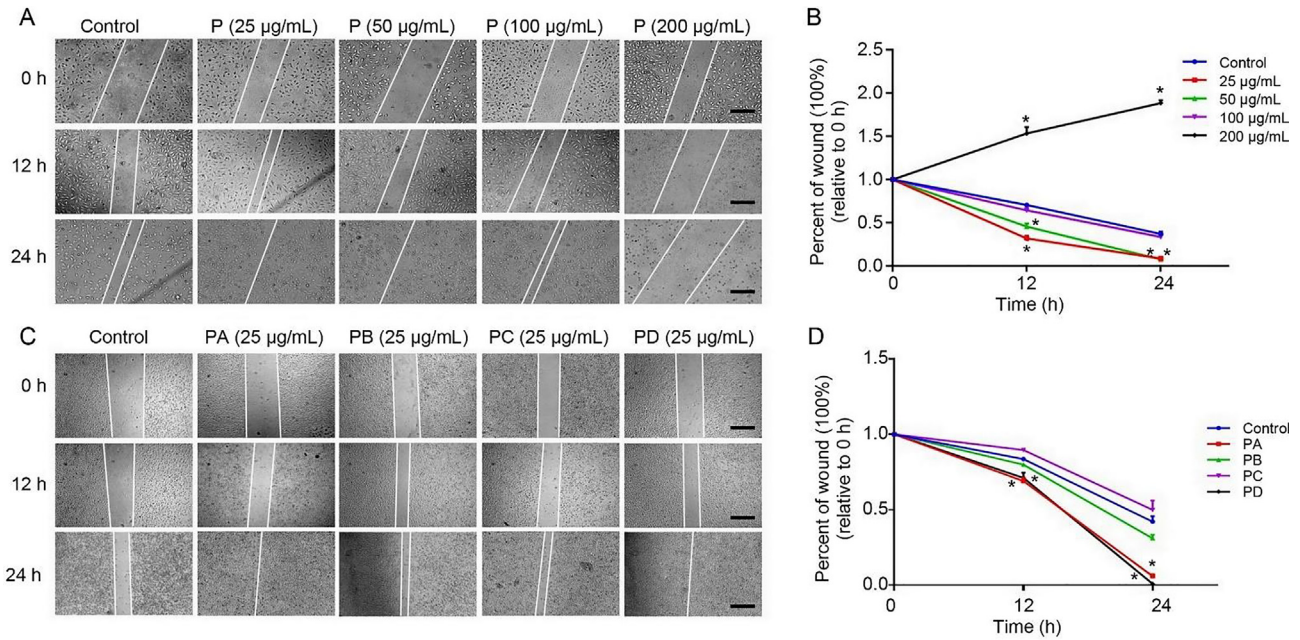


Fig. 5. POL extracts promoted HUVEC cells migration in a concentration-dependent manner. (A) Cells migration process of the control group and P groups with different concentrations ($\times 100$). (B) Percent of the wound to original wound area of each group in Fig. 5A. (C) Cells migration process in control and PA, PB, PC and PD groups ($\times 100$). (D) Percent of wound to original wound area of each group in Fig. 5C. Scale bar: 200 μm . $*P < 0.05$ vs control group. Scale bar: 200 μm . Data presented as means \pm SD.

3.3. Extracts P and PD promoted wound healing in DTPI mice models

The wound area in each group gradually decreased with the extension of treatment time, but the accelerated rate of wound closure was more apparent in the P and PD_M treatment groups (Fig. 6A). After 11 d, the percentage of wound area in the DTPI, P, PD_L, PD_M, and PD_H groups were $(48.19 \pm 3.51)\%$, $(13.54 \pm 3.05)\%$, $(35.49 \pm 3.61)\%$, $(5.53 \pm 2.95)\%$ and $(37.24 \pm 4.73)\%$, respectively ($P < 0.05$) (Fig. 6B). Additionally, after 17 d, the wounds in the P and PD groups appeared to be healed, whereas those in the DTPI group had not healed by day 21 ($P < 0.05$).

3.4. Histopathological evaluation and immunological analysis

As shown in Fig. 7A and B, only wounds in the PD_M group had regenerated epithelial tissue after 7 d. Moreover, the thickness of the regenerated epithelium showed no significant difference between the PD and the normal groups ($P > 0.05$). However, the regenerated epithelium in the DTPI group was significantly thicker than that in treatment groups and the normal group on day 21 ($P < 0.05$).

After 7 d of wound healing, there was significant inflammatory cell infiltration into the wound site in the DTPI group and PD_L group. DTPI caused an increased inflammatory cell infiltration compared to the PD_L group ($P < 0.05$) (Fig. 7A and C). In contrast, there was no visual indication of increased inflammatory cell infiltration in the PD_M and PD_H groups (Fig. 7A). On days 14 and 21, the number of inflammatory cells was significantly reduced in the PD groups compared with the DTPI group ($P < 0.05$) (Fig. 7C). Additionally, there was no significant difference in the number of inflammatory cells between the PD_M group and the normal group on day 14 and 21 ($P > 0.05$).

Next, we calculated the density of skin accessory organs, including sebaceous and sweat glands. Skin accessory organs were first to form in the PD_M group on day 7 (Fig. 7D). Moreover, the skin accessory organ density in the PD_M group remained higher than

that in the DTPI group throughout the wound healing process ($P < 0.05$).

Finally, we evaluated the ability of PD to promote vascular regeneration within the wound site. Once again, the PD_M group demonstrated superior performance and had more blood vessels than the DTPI group at all three-time points ($P < 0.05$) (Fig. 7E). Indeed, only the wounds that received PD_M treatment firstly showed neovascularization on day 7 (Fig. 7A). In addition, we used WB to analyze the expression levels of VEGF-A protein on day 14. Only the PD_M group showed similar expression levels to the normal group ($P > 0.05$), and the VEGF-A expression levels of DTPI, PD_L and PD_H groups were significantly lower than that in the normal group. However, the VEGF-A expression levels in the PD treatment groups were all significantly higher than that in the DTPI group ($P < 0.05$) (Fig. 7F and G).

Collagen deposition was a key feature of granulation tissue required for wound closure. As shown in Fig. 8A, MT staining revealed blue collagen fibres and red muscle fibres. There was a 3-fold increase of collagen deposited within the wounds treated with PD_M ($0.29 \pm 0.03\%$), as compared to the wounds in DTPI group ($0.06 \pm 0.03\%$), PD_L group ($0.10 \pm 0.03\%$) and PD_H group ($0.06 \pm 0.03\%$) on day 7 ($P < 0.05$) (Fig. 8B). Quantification of MMP-9 protein expression on day 14 revealed its overexpression in the DTPI group, which was significantly higher than wounds in the PD_M group ($P < 0.05$) (Fig. 8C and D). PD_M treated wounds had a similar expression level of MMP-9 as the normal group ($P > 0.05$).

3.5. PD suppressed iron accumulation in DTPI wound

Iron overload is a hallmark changed of DTPI. Iron deposited in tissues was stained blue using Perl' stain. Iron aggregates were not visible in the normal and PD_M groups, whereas iron aggregates were extensive in the DTPI group on day 7 and 14 (Fig. 9A). Furthermore, ICP-MS analysis revealed that the iron concentration in the PD_M group was consistently lower than the DTPI group on day 7 and 14 ($P < 0.05$). In addition, there was a 2-fold decrease in

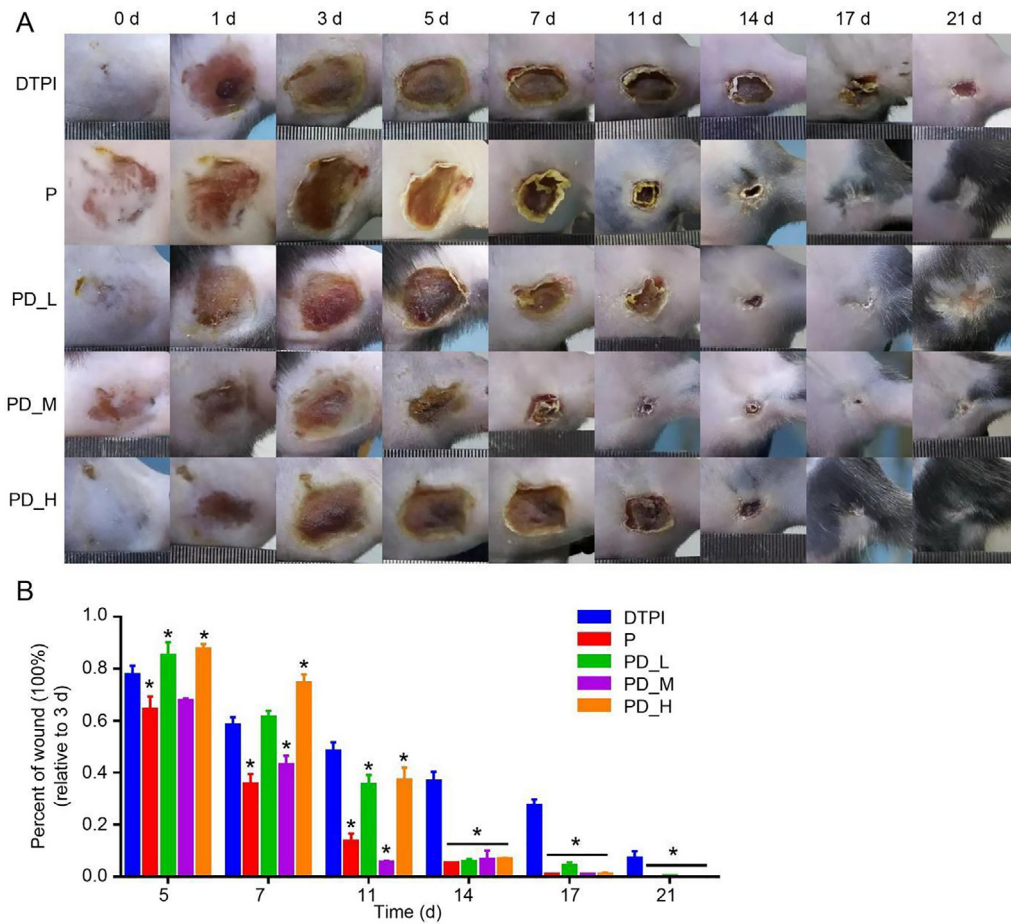


Fig. 6. P and PD treatment accelerated DTPI wound healing. (A) Changes of wound morphology in DTPI, P and different concentrations of PD groups. (B) Quantification of wound proportion in each group. PD_L, PD_M and PD_H concentrations were 3, 6 and 12 mg/mL, respectively. Data presented as means \pm SD. * P < 0.05 vs DTPI group.

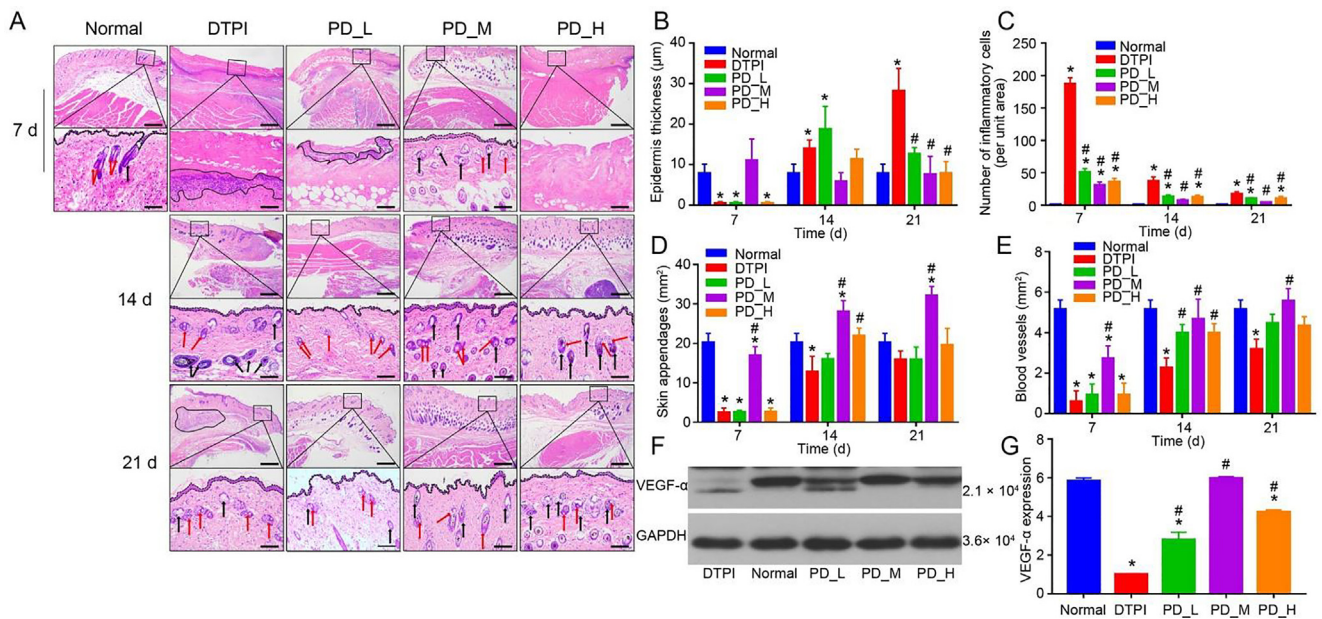


Fig. 7. PD improved the quality of wound healing. PD treatment promoted vascular regeneration and inhibited inflammation. (A) Representative HE staining images of wounds in normal, DTPI, and PD treatment groups. H&E staining showed the border of the epidermal layer (dashed black line outlines), the inflammatory cell infiltration area (solid black line outlines), neonatal blood vessels (red arrows), and skin appendages (black arrows). Scale bar: 40 \times , 500 μ m; 200 \times , 100 μ m. (B) Epidermal thickness, (C) Inflammatory cell density, (D) Skin appendages density, and (E) Blood vessels density of each group. (F) Western blotting analysis of VEGF-A protein expression on 14 d. (G) Quantification of VEGF-A protein expression. Data presented as means \pm SD. * P < 0.05 vs normal group, # P < 0.05 vs DTPI group.

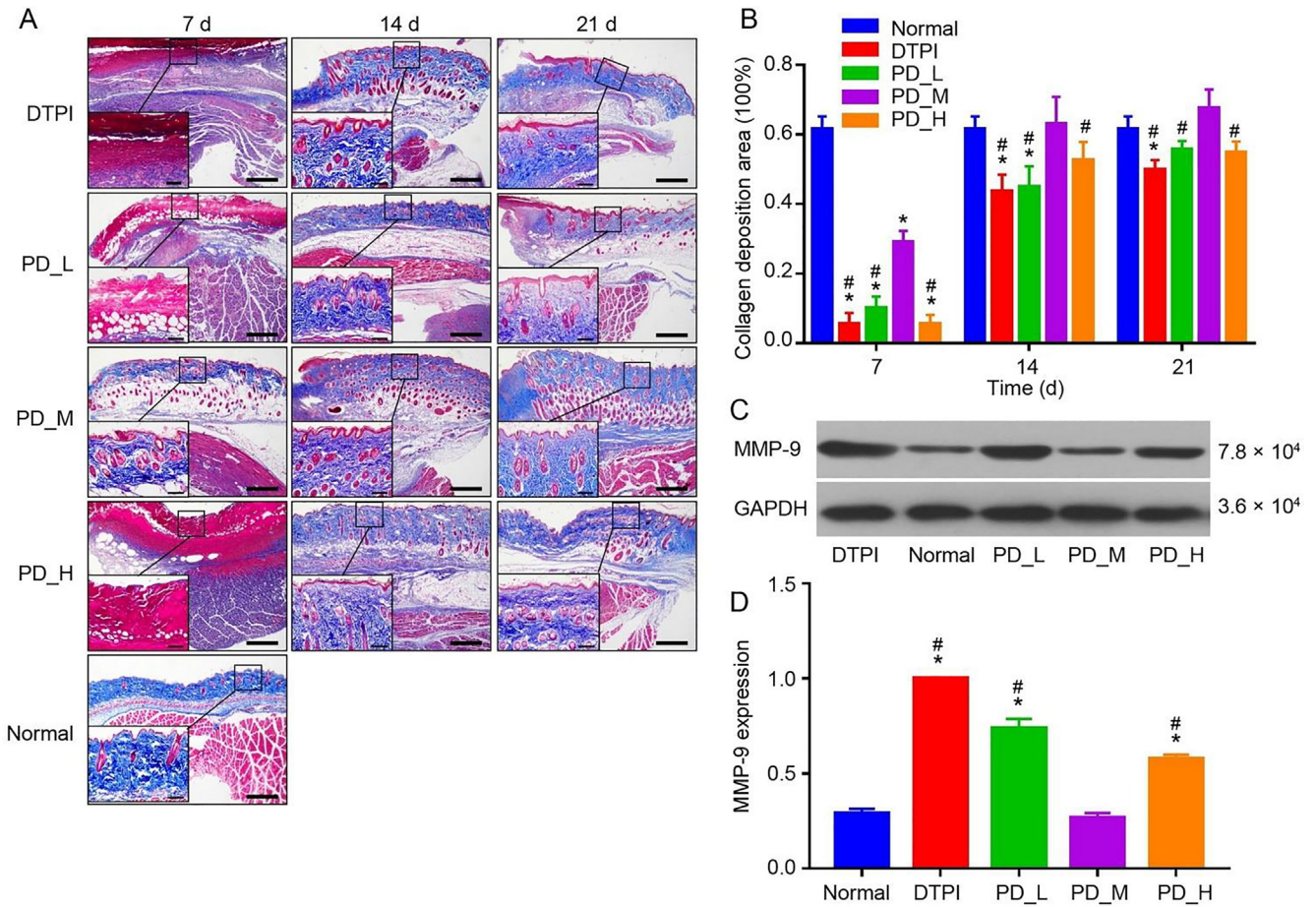


Fig. 8. PD treatment enhanced collagen formation. (A) Representative MT staining images of wounds. (B) Quantification of collagen deposition area. (C) Western blotting analysis of MMP-9 protein expression on 14 d. (D) Quantification of MMP-9 protein expression. **P* < 0.05 vs normal group, #*P* < 0.05 vs DTPI group. Scale bar: 40×, 500 μm; 200×, 100 μm. PD_L, PD_M and PD_H concentrations were 3, 6, and 12 mg/mL, respectively. Data presented as means ± SD.

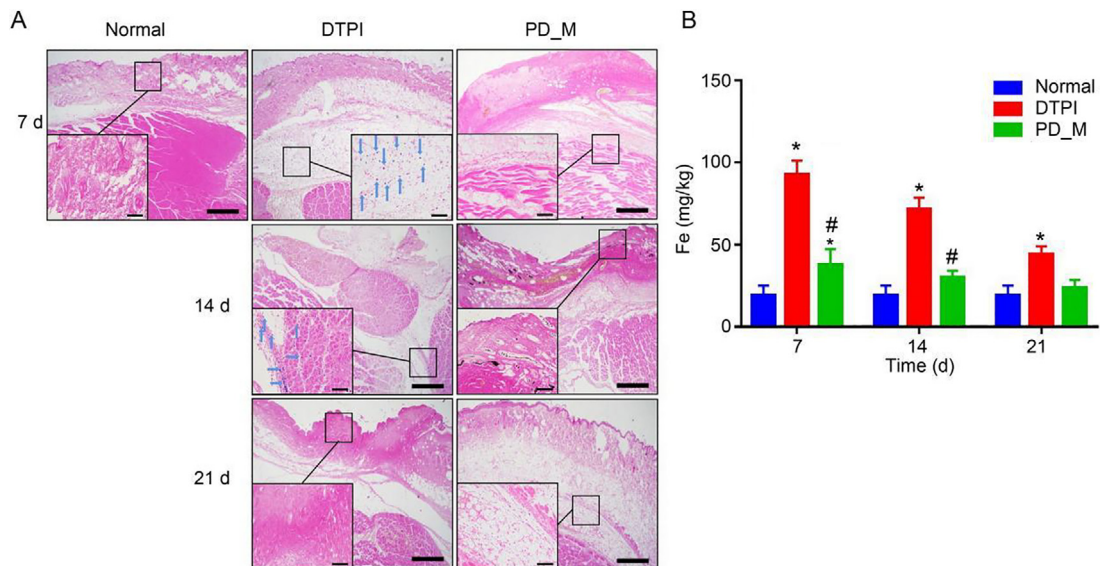


Fig. 9. PD inhibited iron accumulation. (A) Representative Perls' stain images of wounds on 7, 14, and 21 d. Blue arrows indicated the iron deposition on tissue space. (B) Quantification of iron concentration of wound muscle using ICP-MS. Scale bar: 40×, 500 μm; 200×, 100 μm. The concentration of PD_M was 60 mg/mL. Data presented as means ± SD. **P* < 0.05 vs normal group, #*P* < 0.05 vs DTPI group.

PD_M group [(37.7 ± 9.6) mg/kg] compared with the DTPI group [(92.61 ± 8.5) mg/kg] on day 7 (Fig. 9B).

4. Discussion

In traditional medical practice, POL is often used to treat superficial wounds by topical administration. To date, few studies have investigated the link between vascularization and POL in the DTPI model. This study demonstrated that PD prepared for intragastrical administration could promote vascular regeneration, inhibit iron aggregation, and further enhance DTPI wound healing.

DTPI is caused by ischemia–reperfusion, and its healing is hampered by poor vascularization (Saleh et al., 2019). Our *in vitro* experiments demonstrated that all five POL extracts had the remarkable ability to promote HUVEC tube formation and migration, suggesting pro-angiogenic effects of POL extracts. Interestingly, the five extracts showed different activities in promoting HUVEC proliferation, which may be due to the different solvent extracts of POL having different safe concentration ranges and cytocompatibility (Baradaran Rahimi, Mousavi, Haghighi, Soheili-Far & Askari, 2019). In the present study, the PD fraction extract possessed the most robust and reproducible effects on promoting HUVEC proliferation, which may be related to the main bioactive components within PD, such as glycosides and amino acids (Boskabady, Kaveh, Shakeri, Mohammadian Roshan & Rezaee, 2019; Yang et al., 2016).

In our *in vivo* experiments, re-epithelialization first occurred in the PD treated groups, further verifying that the PD fraction had pro-regenerative and beneficial effects on multiple cell types. Furthermore, PD suppressed wound site inflammation. On the one hand, the inflammatory cell numbers within the PD group were fewer than that in the DTPI group; on the other hand, the expression of MMP-9 was only lowered in the PD_M group. Previous studies have confirmed that overexpression of MMP-9 was an indicator of muscular inflammation and was related to poor wound healing outcomes (Tabandeh, Oryan & Mohammadipour, 2014; Wang et al., 2018). Hence, our results suggested that PD_M treatment could effectively inhibit wound site inflammation whilst promoting regenerative activities in non-immune cell types. These findings concur with recent data that showed POL had anti-inflammatory potential through the partial suppression of NF-κB and MAPK activation (Miao et al., 2019).

Furthermore, the number of neo-vessels and VEGF-A expression level suggested that PD promoted vascular regeneration *in vivo*. This finding also was confirmed *in vitro* experiments. Our data concurred with a previous study, wherein POL was shown to promote pro-angiogenic activity *in vitro* (Baradaran Rahimi, Mousavi, Haghighi, Soheili-Far & Askari, 2019). Moreover, DTPI wounds in the PD_M group were faster regenerating hair follicles, sebaceous glands, and sweat glands with the most considerable density. Hair follicle growth areas have been suggested to promote wound healing in the surrounding tissue area. Thus, rapid attainment of regenerated hair follicles would theoretically support the improved quality of wound healing (Bhoopalam, Garza & Reddy, 2020; Guerrero-Juarez et al., 2019).

Similarly, the deposition and ordered arrangement of collagen are necessary for high-quality wound healing. Our *in vivo* work confirmed previous reports that POL extract up-regulated type I collagen production and down-regulated MMPs (Du et al., 2021). Here, we demonstrated that PD_M treatment resulted in the highest production of collagen ECM and lowest expression of MMP-9 compared with the DTPI and treated groups.

Previous studies have found that iron deposits exist in tissues and macrophages of chronic wounds. The wounds with increased

iron deposition fail to induce the switch from pro-inflammatory M1 to anti-inflammatory M2 macrophages and fail to potentiate pro-inflammatory cytokines and chemokines production (TNF-α, IL-1β), thus delaying wound healing (Sindrilaru & Scharffetter-Kochanek, 2013). This study hypothesized that DTPI wounds might also have iron accumulation, much like other chronic wounds (Vander Beken et al., 2019). PD treatment inhibited iron deposition, but the mechanism of action remained unknown. Our identification of iron overload existing in DTPI provided new insights into DTPI pathology and potential routes for treatment.

These findings suggest that PD is an alternative medicine to promote DTPI wound healing. Future studies defining the mechanism of PD inhibiting inflammation and iron deposition are essential to progress DTPI treatment and healthcare development.

5. Conclusion

In summary, our research demonstrated that PD could promote DTPI wound healing by enhancing angiology regeneration and inhibiting iron accumulation for the first time. We highlight the unique advantage of POL over other existing treatments for DTPI. Overall, PD extract offers a practical and alternative medicine for DTPI wound therapy.

Declaration of Competing Interest

The authors declare that they have no known competing financial interests or personal relationships that could have appeared to influence the work reported in this paper.

Acknowledgements

We thank the Chinese Academy of Medical Sciences & Peking Union Medical College Institute of Biomedical Engineering for donating HUVEC cells.

This work was supported by the Youth Program of the National Natural Science Foundation of China [grant No. 8170, 1838].

References

- Alves, F. M., Kysenius, K., Caldwell, M. K., Hardee, J. P., Crouch, P. J., Ayton, S., ... Koopman, R. (2021). Iron accumulation in skeletal muscles of old mice is associated with impaired regeneration after ischaemia-reperfusion damage. *Journal of Cachexia, Sarcopenia and Muscle*, 12(2), 476–492.
- Baradaran Rahimi, V., Mousavi, S. H., Haghighi, S., Soheili-Far, S., & Askari, V. R. (2019). Cytotoxicity and apoptogenic properties of the standardized extract of *Portulaca oleracea* on glioblastoma multiforme cancer cell line (U-87): A mechanistic study. *EXCLI Journal*, 18, 165–186.
- Bhoopalam, M., Garza, L. A., & Reddy, S. K. (2020). Wound induced hair neogenesis – A novel paradigm for studying regeneration and aging. *Frontiers in Cell and Developmental Biology*, 8, 582346.
- Black, J. M., & Berke, C. T. (2020). Deep tissue pressure injuries: Identification, treatment, and outcomes among critical care patients. *Critical Care Nursing Clinics of North America*, 32(4), 563–572.
- Boskabady, M. H., Kaveh, M., Shakeri, K., Mohammadian Roshan, N., & Rezaee, R. (2019). Hydro-ethanolic extract of *Portulaca oleracea* ameliorates total and differential WBC, lung pathology and oxidative biomarkers in asthmatic rats. *Iranian Journal of Pharmaceutical Research*, 18(4), 1947–1958.
- Du, C., Li, Y., Xia, X., Du, E., Lin, Y., Lian, J., ... Qin, Y. (2021). Identification of a novel collagen-like peptide by high-throughput screening for effective wound-healing therapy. *International Journal of Biological Macromolecules*, 173, 541–553.
- Frykberg, R. G., & Banks, J. (2015). Challenges in the treatment of chronic wounds. *Advances in Wound Care*, 4(9), 560–582.
- Guerrero-Juarez, C. F., Dedhia, P. H., Jin, S., Ruiz-Vega, R., Ma, D., Liu, Y., ... Plikus, M. V. (2019). Single-cell analysis reveals fibroblast heterogeneity and myeloid-derived adipocyte progenitors in murine skin wounds. *Nature Communications*, 10(1), 650.
- Iranshahi, M., Javadi, B., Iranshahi, M., Jahanbakhsh, S., Mahyari, S., Hassani, F., & Karimi, G. (2017). A review of traditional uses, phytochemistry and pharmacology of *Portulaca oleracea* L. *Journal of Ethnopharmacology*, 205, 158–172.

- Jensen, P. D., Nielsen, A. H., Simonsen, C. W., Baandrup, U. T., Jensen, S. E., Bøgsted, M., ... Kjaergaard, B. (2021). In vivo calibration of the T2* cardiovascular magnetic resonance method at 1.5 T for estimation of cardiac iron in a minipig model of transfusional iron overload. *Journal of Cardiovascular Magnetic Resonance*, 23(1), 27.
- Lee, J. I., Oh, J. H., Kong, C. S., & Seo, Y. (2019). Evaluation of anti-adipogenic active homoioflavonoids from *Portulaca oleracea*. *Zeitschrift für Naturforschung C, Journal of Biosciences*, 74(9–10), 265–273.
- Liu, P., Yang, X., Han, J., Zhao, M., Guo, J., Si, R., ... Zhang, J. (2020). Tazarotene-loaded PLGA nanoparticles potentiate deep tissue pressure injury healing via VEGF-Notch signaling. *Materials Science & Engineering C, Materials for Biological Applications*, 114 111027.
- Mekonnen, A., Sidamo, T., Asres, K., & Engidawork, E. (2013). In vivo wound healing activity and phytochemical screening of the crude extract and various fractions of *Kalanchoe petitiiana* A. Rich (Crassulaceae) leaves in mice. *Journal of Ethnopharmacology*, 145(2), 638–646.
- Meng, J., Liu, Y., Han, J., Tan, Q., Chen, S., Qiao, K., ... Yang, C. (2017). Hsp90 β promoted endothelial cell-dependent tumor angiogenesis in hepatocellular carcinoma. *Molecular Cancer*, 16(1), 72.
- Miao, L., Tao, H., Peng, Y., Wang, S., Zhong, Z., El-Seedi, H., ... Xiao, J. (2019). The anti-inflammatory potential of *Portulaca oleracea* L. (purslane) extract by partial suppression on NF- κ B and MAPK activation. *Food Chemistry*, 290, 239–245.
- Pakdel, R., Vatanchian, M., Niazmand, S., Beheshti, F., Rahimi, M., Aghaee, A., & Hadjzadeh, M. A. (2019). Comparing the effects of *Portulaca oleracea* seed hydroalcoholic extract, valsartan, and vitamin E on hemodynamic changes, oxidative stress parameters and cardiac hypertrophy in thyrotoxic rats. *Drug and Chemical Toxicology*, 1–8.
- Preston, A., Rao, A., Strauss, R., Stamm, R., & Zalman, D. (2017). Deep tissue pressure injury: A clinical review. *The American Journal of Nursing*, 117(5), 50–57.
- Qiao, J. Y., Li, H. W., Liu, F. G., Li, Y. C., Tian, S., Cao, L. H., ... Miao, M. S. (2019). Effects of *Portulaca oleracea* extract on acute alcoholic liver injury of rats. *Molecules (Basel, Switzerland)*, 24(16).
- Rashed, A., Afifi, F., & Disi, A. (2003). Simple evaluation of the wound healing activity of a crude extract of *Portulaca oleracea* L. (growing in Jordan) in *Mus musculus* JVI-1. *Journal of Ethnopharmacology*, 88, 131–136.
- Saleh, B., Dhaliwal, H. K., Portillo-Lara, R., Shirzaei Sani, E., Abdi, R., Amiji, M. M., & Annabi, N. (2019). Local Immunomodulation using an adhesive hydrogel loaded with miRNA-laden nanoparticles promotes wound healing. *Small*, 15(36) e1902232.
- Sindrilaru, A., & Scharffetter-Kochanek, K. (2013). Disclosure of the culprits: Macrophages-versatile regulators of wound healing. *Advances in Wound Care (New Rochelle)*, 2(7), 357–368.
- Tabandeh, M. R., Oryan, A., & Mohammadalipour, A. (2014). Polysaccharides of Aloe vera induce MMP-3 and TIMP-2 gene expression during the skin wound repair of rat. *International Journal of Biological Macromolecules*, 65, 424–430.
- Tao, H., Ye, D. L., Wu, Y. L., Han, M. M., Xue, J. S., Liu, Z. H., ... Wang, H. L. (2018). The protective effect of polysaccharide extracted from *Portulaca oleracea* L. against Pb-induced learning and memory impairments in rats. *International Journal of Biological Macromolecules*, 119, 617–623.
- Vander Beken, S., de Vries, J. C., Meier-Schiesser, B., Meyer, P., Jiang, D., Sindrilaru, A., ... Scharffetter-Kochanek, K. (2019). Newly defined ATP-binding cassette subfamily B Member 5 positive dermal mesenchymal stem cells promote healing of chronic iron-overload wounds via secretion of interleukin-1 receptor antagonist. *Stem Cells (Dayton, Ohio)*, 37(8), 1057–1074.
- Vogt, T. N., Koller, F. J., Santos, P. N. D., Lenhani, B. E., Guimarães, P. R. B., & Kalinke, L. P. (2020). Quality of life assessment in chronic wound patients using the Wound-QoL and FLQA-Wk instruments. *Investigacion y Educacion en Enfermeria*, 38(3).
- Wang, W., Liu, Y., You, L., Sun, M., Qu, C., Dong, X., ... Ni, J. (2020). Inhibitory effects of Paris saponin I, II, VI and VII on HUVEC cells through regulation of VEGFR2, PI3K/AKT/mTOR, Src/eNOS, PLC γ /ERK/MERK, and JAK2-STAT3 pathways. *Biomedicine & Pharmacotherapy*, 131 110750.
- Wang, W., Yang, C., Wang, X. Y., Zhou, L. Y., Lao, G. J., Liu, D., ... Ren, M. (2018). MicroRNA-129 and -335 promote diabetic wound healing by inhibiting Sp1-mediated MMP-9 expression. *Diabetes*, 67(8), 1627–1638.
- Yang, X., Yan, Y., Li, J., Tang, Z., Sun, J., Zhang, H., ... Liu, L. (2016). Protective effects of ethanol extract from *Portulaca oleracea* L. on dextran sulphate sodium-induced mice ulcerative colitis involving anti-inflammatory and antioxidant. *American Journal of Translational Research*, 8(5), 2138–2148.
- Zheng, G., Mo, F., Ling, C., Peng, H., Gu, W., Li, M., & Chen, Z. (2018). *Portulaca oleracea* L. alleviates liver injury in streptozotocin-induced diabetic mice. *Drug Design, Development and Therapy*, 12, 47–55.
- Zhou, Y., Xin, H., Rahman, K., Wang, S., Peng, C., & Zhang, H. (2015). *Portulaca oleracea* L.: A review of phytochemistry and pharmacological effects. *BioMed Research International*, 2015, 925631.